Supplementary Information

1 Electro-osmotic flow

Electro-osmotic flow is proportional to the applied electric field.[1] As shown in the cross-sectional view in Fig. 1, the applied field moves the counter-ions in the Debye layer at the interface of the device and the fluid (in our experiments, the fluid is water). The motion of the counter-ions moves the rest of the fluid due to viscous drag with the flow velocity being directly proportional to the applied electric field.

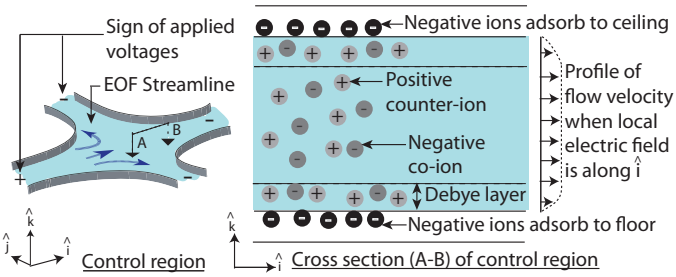

Fig. 1 The left panel shows the streamlines of the flow following the applied electric field. The flow profile in the device (along section A-B of the left panel) is shown in the right panel.[1] The naturally occurring negatively charged ions adsorbed to the surface of the device are shielded by positively charged ions from the fluid. The ions in the thin diffuse (Debye) layer near the device-fluid interface move under the influence of the electric field and drag the rest of the fluid by viscous forces.[1] The resulting electro-osmotic flow profile is uniform along $\hat{k}$ (except for the variation in the thin Debye layer, not drawn to scale) with the flow velocity proportional to the applied electric field. Objects like NWs that are suspended in the fluid are entrained in this flow.

Spatio-temporal variations of the applied electric field pattern moves the carpet of counter-ions, and consequently the fluid, along that pattern, translating an immersed object over any desired path in the same way that moving a carpet in a room results in the movement of furniture placed on it. EOF is irrotational (staying with the analogy, rotating the carpet is disallowed) because the underlying electric field is curl-free. An immersed object needs to be less symmetric than a sphere (for example, rod-shaped) for EOF shear to be able to rotate it.[2,3]

2 Estimating the center of mass and orientation of NW

The center of mass (x_{cm}, y_{cm}) of the NW in every feedback update was found by thresholding on the pixel brightness. In every update a square window, 45 pixels on a side, centered around the previous center of mass estimate was considered for image processing (this window was found to be large enough to accommodate the largest possible translation of the NW in the previous update). Every contiguous set of sufficiently bright pixels in this window was considered as a possible contender of the NW image, with a pixel declared as sufficiently bright if it was at least 40% as bright as the brightest pixel in the window. The center of mass of each of these contenders was computed, with the true NW center of mass (x_{cm}, y_{cm}) declared as the one which was closest to the center of mass estimate in the previous feedback update. The set S_{NW} of sufficiently bright contiguous pixels, with coordinates (x_i, y_i), having center of mass (x_{cm}, y_{cm}) was declared as the current image of the NW.

The orientation θ of the NW, defined to lie in the range $R_{\frac{\pi}{2}} = (\frac{-\pi}{2}, \frac{\pi}{2}]$, was then estimated as the orientation of the line passing through (x_{cm}, y_{cm}) that was a least-squares best fit to the pixels in the set S_{NW} that comprised the NW image. The orientation θ of the NW should then, due to the fit, satisfy

$$\tan(2\theta) = \frac{2\langle x_i y_i \rangle}{\langle y_i^2 \rangle - \langle x_i^2 \rangle} \quad (1)$$

where (x_i, y_i) are the pixel co-ordinates measured with respect to the origin (x_{cm}, y_{cm}) and $\langle . \rangle$ denotes the averaging operator. Thus the orientation θ of the NW can be obtained by using Eqn. 1 with two caveats:
(1) If $\langle y_i^2 \rangle = \langle x_i^2 \rangle$ then $\theta = \pm\frac{\pi}{4}$. This ambiguity was resolved by declaring $\theta = \frac{\pi}{4}$ if $\langle x_i y_i \rangle > 0$ and $\theta = -\frac{\pi}{4}$ otherwise.
(2) Even if $\langle y_i^2 \rangle \neq \langle x_i^2 \rangle$, Eqn. 1 gives two possible choices for θ since $\tan(2\theta) = \tan(2\theta - \pi)$. In this case, exactly one of these choices lies in the range $R_{\frac{\pi}{4}} = (\frac{-\pi}{4}, \frac{\pi}{4})$. The NW orientation was declared to lie in $R_{\frac{\pi}{4}}$ if $\langle x_i^2 \rangle > \langle y_i^2 \rangle$ and in $(R_{\frac{\pi}{2}} - R_{\frac{\pi}{4}})$ if $\langle x_i^2 \rangle < \langle y_i^2 \rangle$.

3 Measurement of median angular velocity and rotational diffusion coefficient

We first describe the measurement of the median NW angular velocity imparted by electro-osmotic flow control (EOFC) during the trapping phase of the experiment (when the NW is held at a fixed position and orientation) for the three (SU8, Si and Au) NWS. We then describe the measurement of the rotational diffusion coefficient D_θ for the three NWs.

For measuring the median angular velocity, we first estimated a list $\{\omega(i)\}$ of EOFC-imparted NW angular velocities during each feedback update i of the trapping phase. For each i we substitute the applied experimental voltages, and the measured NW position and orientation values in an EOF-physics based map relating the NW angular velocity to the applied

voltages (see Eqn. 7 of previous work[3]) to get $\{\omega(i)\}$. The zeta potential magnitude at the device-fluid interface used in this estimate was[4] 50 mV, viscosity of water was[5] 8.9×10^{-4} Pa.s and relative dielectric permittivity of water was[5] 80. For each NW, the median of $\{\omega(i)\}$ is estimated to be the angular velocity ω that is available to combat rotational diffusion.

We measured D_θ for each of the three same objects that were trapped by measuring their mean square rotational displacements when they were each allowed to freely move after the trapping experiments. Each object was tracked until it drifted to the edge of the control region. In the manner described in Rose et al.,[6] the orientation of the objects were fit using linear regression to the additive diffusion/noise model $\langle\theta^2_{exp}\rangle = 2D_\theta t + \langle\theta^2_{meas}\rangle$, where $\langle\theta^2_{exp}\rangle$ is the mean squared deviation of the experimentally measured rotation and $\langle\theta^2_{meas}\rangle$ is the mean squared measurement noise (the justification for such an additive noise model for diffusional motion of colloids is detailed in Crocker et al.[7]). This was repeated at least three times per object (once it reached the edge of the control region, the NW was brought back towards the center of the center of the control region (by EOF) and allowed to freely move once again). The rotational diffusion coefficients, fitted to the additive diffusion model, and averaged over the multiple experiments were measured to be $6\pm2\times10^{-3}$ rad^2/s for the SU8 rod, $4\pm1\times10^{-3}$ rad^2/s for the SiNW and $8\pm2\times10^{-3}$ rad^2/s for the AuNW. The measurement noises were measured to be 0.02 rad, 0.01 rad and 0.06 rad respectively.

4 Motion due to residual pressure flow

The fluid in the reservoirs of our device experience an unbalanced surface tension that creates a background residual pressure flow that perturbs NW motion. This perturbation, compensated by EOFC, becomes evident when control is switched off as is the case while measuring D_θ.

The perturbation has a significant translatory effect on the NW motion as can be seen by the almost linear graph of the translational displacement in Fig. 2 (a stochastic translational diffusion component negligibly adds to the linear component). The strength of the NW translation due to residual pressure flow can be compared to that of Brownian translation by comparing transit times in the control region. As seen in Fig. 2, the SU8 rod was transported by a distance of 75 μm to the edge of the control region within $\approx$ 30 s due to the residual pressure flow (so v_{press}, the translational velocity due to residual pressure flow, is less than 3 μm/s - we use v_{press} to estimate the effect of induced charge electrophoresis in the next section). Without the residual pressure flow, translational diffusion by itself would have required $>$ 9000 s to move the rod by the same distance.[8]

However, as shown in Fig. 2, the stochastic nature of the *rotational* Brownian motion is *not* affected by the residual pressure flow. For comparison, a 10 μm $\times$1 μm cylindrical rod in water at room temperature, far from the device walls, has a theoretical rotational diffusion coefficient of 8.4×10^{-3} rad^2/s.[9] The proximity of the rod to the floor of the device is responsible[10] for the ($\approx$25%) lower experimental values mentioned above. The lower values show that the residual pressure flow does not significantly add to the rotational mean squared deviations used to estimate D_θ.

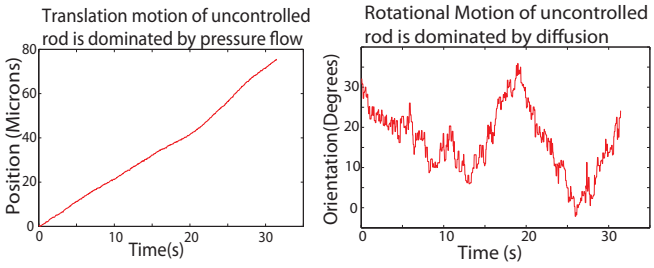

Fig. 2 Rotational displacements of an uncontrolled SU8 rod is dominated by rotational diffusion but its translation is dominated by residual pressure flow.

5 Other forces affecting NW motion

Induced charge electrophoresis (ICEP) due to the applied electric field can have a perturbatory effect on NW motion. ICEP affects rotational,[13] but not translational, motion of nanowires in an electric field. We compare the angular velocities due to ICEP and EOF in the following. The angular velocity ω_{ICEP} due to ICEP, can be bounded by $\omega_{ICEP} \leq \frac{\varepsilon E^2}{6\mu}$ (see SI of our previous work[3]) where μ and ε are the viscosity (8.9×10^{-4} Pa.s) and relative dielectric permittivity (80) of water[5] respectively and E is the magnitude of the local electric field strength. The local electric field strength in our device is spent on countering translation, while the electric field gradient is spent on countering rotation. Since the translation being countered is mostly due to residual pressure flow, the magnitude of the electric field strength needed to counter it using EOF is $E = \frac{v_{press}\mu}{\varepsilon\zeta}$, where the magnitude of the zeta potential at the device-fluid interface is[4] $\zeta = 50$ mV and v_{press} is the translational velocity due to residual pressure flow that is being countered by EOF. Since $v_{press} < 5$ μm/s in our experiments, we get after substituting values, $\omega_{ICEP} \leq 2\times10^{-3}$ rad/s. This is less than 3.5 % of the median rotational velocity of the NWs observed in our experiments. Thus we conclude that ICEP negligibly affects NW rotational velocity in our device.

References

1 R.F. Probstein, *Physicochemical Hydrodynamics*, New York, Wiley, 1994.

2 H. Brenner, "The Stokes resistance of an arbitrary particle - Part IV. Arbitrary fields of flow" *Chemical Engineering Science*, 19, pp. 703-727, 1964.

3 P. P. Mathai, A. J. Berglund, J. A. Liddle and B. Shapiro, "Simultaneous Positioning and Orientation of a Single Nano-object by Flow Control: Theory and Simulations," *New Journal of Physics*, 13, 013027, 2011.

4 M. D. Armani, S. V. Chaudhary, R. Probst, and B. Shapiro, "Using feedback control of microflows to independently steer multiple particles," *Journal of Microelectromechanical Systems*, 15, 4, pp. 945-954, August 2006.

5 D. R. Lide (Editor-in-chief) *CRC handbook of Chemistry and Physics*, CRC press, Ed. 90, 2009.

6 K. A. Rose, J. A. Meier, G. M. Dougherty, J. G. Santiago, "Rotational Electrophoresis of Striped Metallic Microrods," *Physical Review E*, 75, 011503:1-15, 2007.

7 J. C. Crocker and D. G. Grier, "Methods of Digital Video Microscopy for Colloidal Studies," *Journal of Colloid Interface Science*, 179, pp.298-310, 1996.

8 The translational diffusion coefficients perpendicular and parallel to the long axis of a cylindrical rod[11] are $D_\perp = \frac{kT\cdot(log(2l/d)+0.5)}{4\pi\eta l} = 0.13\ \mu\text{m}^2/\text{s}$ and $D_\parallel = \frac{kT\cdot(log(2l/d)-0.5)}{2\pi\eta l} = 0.18\ \mu\text{m}^2/\text{s}$ respectively for the SU8 rod immersed in water at room temperature, where l is the length of the rod, d is the diameter, k is the Boltzmann constant, T is the temperature, η is the dynamic viscosity of water. A root mean squared displacement of 75 μm due to translational diffusion alone would thus require 9072 s on average.

9 $D_\theta = \frac{3kT}{\pi\eta l^3}(log(l/d) + log(4) - 11/16)$ where l is the length of the rod, d is the diameter, k is the Boltzmann constant, T is the temperature, η is the dynamic viscosity of water. See derivation in: H. Yamakawa, "Viscoeleastic Properties of Straight Cylindrical Macromolecules in Dilute Solution," *Macromolecules*, 8, 3, pp.339-342, 1975.

10 J. T. Padding and W. J. Briels, "Translational and rotational friction on a colloidal rod near a wall," *The Journal of Chemical Physics*, 132, pp. 054511-1:8, 2010.

11 J. Happel and H. Brenner, *Low Reynolds Number Hydrodynamics*, Englewood Cliffs, Prentice Hall, 1965.

12 A. Sellier, "A note on the electrophoresis of a uniformly charged particle," *Quarterly Journal of Mathematics and Applied Mechanics*, 55, 4, pp.561-572, 2002.

13 D. Saintillan, E. Darve, and E. S. G. Shaqfeh, "Hydrodynamic Interactions in the induced-charge electrophoresis of colloidal rod suspensions," *Journal of Fluid Mechanics*, 563, pp.223-259, 2006.